Modern Physics Letters B, Vol. 17, Nos. 10, 11 & 12 (2003) 549–558

World Scientific
www.worldscientific.com

# HOT-ELECTRON INSTABILITY IN SUPERCONDUCTORS

MILIND N. KUNCHUR* and JAMES M. KNIGHT

*Department of Physics and Astronomy*
*University of South Carolina, Columbia, SC 29208, U.S.A.*
**kunchur@sc.edu*
*http://www.physics.sc.edu/kunchur*

High flux velocities in a superconductor can distort the quasiparticle distribution function and elevate the electronic temperature. Close to $T_c$, a non-thermal distribution function shrinks the vortex core producing the well-known Larkin-Ovchinnikov flux instability. In the present work we consider the opposite limit of low temperatures, where electron-electron scattering is more rapid than electron-phonon, resulting in an electronic temperature rise with a thermal-like distribution function. This produces a different kind of flux instability, due to a reduction in condensate and expansion of the vortex core. Measurements in YBCO films confirm the distinct predictions ofthis mechanism.

*Keywords*: Flux; vortex; superconductor; superconductivity.

PACS Number(s): 74.60.Ge, 74.72.Bk, 71.10.Ca, 71.38.-k, 72.10.Di, 72.15.Lh, 73.50.Fq

## 1. Introduction

A physical system in a stable steady state has a balance between forces such that a small change in one force results in a restorative change in the others, leading to a new stable state of the system. An object dragged through a viscous liquid by an external driving force balanced by a drag force represents such a system. An increase in the driving force causes an increase in velocity and the opposing drag, resulting in negative feedback and restabilization. A peculiar situation can arise when the heat generated by the dragged object reduces the viscous coefficient — as in the case of honey — to such an extent that the drag force diminishes with increasing velocity. The motion then becomes unstable and will run away to a higher velocity. Here we have observed an analogous effect in the motion of quantized magnetic vortices in a superconductor, where superheating of the electron gas weakens the condensate and diminishes the viscous drag. This leads to a negative current-voltage slope and an instability.

*Corresponding author.

## 2. Vortex Viscosity in the Linear Regime

When a type II superconductor is subjected to magnetic fields between the lower critical value $H_{c1}$ and upper critical field $H_{c2}$, the system enters the mixed state forming flux vortices containing a quantum of flux $\Phi_o = h/2e$. The superconducting order parameter $\Delta$ is suppressed in the core of the vortex over the length scale of the superconducting coherence length $\xi$ and the core is surrounded by circulating supercurrents. Here we have superconducting films in a perpendicular applied flux density $B$, with a transport electric current density $j$ in the plane of the film. $j$ exerts a Lorentz driving force $F_L = j\Phi_o$ on the vortices and the consequent vortex motion generates an electric field $E = vB$. The motion is opposed by a viscous drag $\eta v$, where $\eta$ is the coefficient of viscosity and $v$ the vortex velocity. In steady state $j\Phi_o = \eta v$ and the response is Ohmic. Larkin and Ovchinnikov (1986) have shown that a dirty superconductor at low temperatures has a free-flux-flow resistivity related to the normal-state value $\rho_n$ by[1]

$$\rho_f/\rho_n \simeq 0.9B/H_{c2}(T)\,. \tag{1}$$

Approximately the same result, without the precise 0.9 prefactor, can be obtained by considering the Ohmic dissipation in the core and temporal changes in the order parameter leading to irreversible entropy transfer[2]; the result is also valid for *d*-wave superconductors that are not superclean.[3] Equation (1) is equivalent to $\eta \approx \Phi_0 H_{c2}/\rho_n$. At low levels of $j$ and $E$, in the assumed dirty limit $l \ll \xi E_F/kT_c$ ($l$ is the mean free path and $E_F$ is the Fermi energy), $\eta$ is a constant that is proportional to the order parameter $\Delta$ and inversely proportional to the size $\sim \xi^2$ (where $\xi$ is the coherence length) of the vortex.[4] (The Hall effect and transverse component of $E$ are negligible for this discussion, as is vortex pinning because of the large driving forces.[5])

## 3. Non-linear Flux Flow

### 3.1. *Earlier work*

At high electric fields and dissipation levels sufficient to alter the electronic distribution function and/or the electronic temperature, $j(E)$ becomes non-linear and can develop an unstable region ($dj/dE < 0$) above some critical vortex velocity $v^*$. For the regime near $T_c$, such an instability has been predicted by Larkin and Ovchinnikov (LO),[6] and has been experimentally well established.[7–10] At high temperatures, the electron-phonon ($ep$) scattering time $\tau_{ep}$ can be shorter than the electron-electron ($ee$) scattering time $\tau_{ee}$, preventing internal equilibration of the electronic system and producing a peculiar non-thermal distribution function. Since the order parameter $\Delta$ is especially sensitive to the distribution function when close to $T_c$, even moderate values of $E$ can sufficiently distort $\Delta$ (via the Eliashberg mechanism[11]) causing a shrinkage of the vortex core and a removal of quasiparticles from its vicinity. This is the gist of the LO behavior.[6,7] As LO themselves emphasize, the effect is most favorable close to $T_c$ for superconductors with a full

gap and, as shown by Bezuglyj and Shklovskij,[12] is dominant for $B < B_T$ (with $B_T \sim 0.1$ T for our low-$T$ regime). One of the predictions of the standard LO effect is a $v^*$ that is $B$ independent. This has been confirmed in $Y_1Ba_2Cu_3O_{7-\delta}$ in the high-$T$ range.[9,10]

### 3.2. *Theoretical model for the hot-electron instability*

Here we investigate the opposite regime of $T \ll T_c$ and $B > B_T$, where $\Delta$ is not sensitive to small changes in the distribution function.[a] Furthermore because $\tau_{ee} < \tau_{ep}$ as $T \to 0$, the distribution function retains a near thermal character and the electronic system suffers mainly a temperature shift with respect to the lattice.[6,12,14,15] Then instead of the standard LO picture described earlier, we consider a more transparent scenario where the main effect of the dissipation is to raise the electronic temperature, create additional quasiparticles, and diminish $\Delta$. The vortex expands rather than shrinks, and the viscous drag is reduced because of a softening of gradients of the vortex profile rather than a removal of quasiparticles. This sequence of events is almost opposite to the standard LO picture and represents a new type of unstable regime prevalent at $T \ll T_c$. All experimental measurables can be calculated without ambiguity, and the predicted field dependencies and full $j(E)$ curves fit the experimental results without any adjustable parameters.

Previously some deviations from LO behavior at intermediate temperatures — such as a $B$-dependent $v^*$ — were treated through modifications to the LO effect, such as an intervortex spacing $l_\phi$ that exceeds the energy-relaxation length $l_\epsilon$[16] or by inclusion of thermal effects.[12,14] Those treatments do not apply to the present $T \ll T_c$ regime where $l_\epsilon \sim \sqrt{D\tau_{ep}} \sim$ 100–1000 nm is larger than $l_\phi = 1.075\sqrt{\Phi_o/B} \sim$ 10–50 nm ($D = 3 \times 10^{-4}$ m$^2$/s is the diffusion constant[9]).

Starting from the $T \sim 0$ limit, the total input power $jE$ travels from electrons to lattice and from there to the bath, so that $T_0 < T_p < T'$, where $T_0$ and $T_p$ are the bath and phonon temperatures, and $T'$ is the raised non-equilibrium electronic temperature. Macroscopic heating, represented by $T_p - T_0 = R_{th}jE$, is $< 5\%$ of the total increase $T'$- $T_0$ for the worst case dissipation so that $T_p \approx T_0$ (Here $R_{th} \sim 1$ nK.cm$^3$/W is the total thermal resistance between the film and the bath; see experimental section. It will be seen later that the specific-heat integral heavily weights the higher temperatures, so that $T_p - T_0$ is quite negligible.). The energy relaxation between electrons and lattice occurs by inelastic *ep* scattering, and is characterized by an effective time $\tau_\epsilon \sim \langle\tau_{ep}\rangle$. The principal contributions to $\rho_n$ come from impurities and phonons. Since the phonon temperature remains near the bath temperature, the value of $\rho_n$ will not change as the non-equilibrium $T'$ rises. Thus putting $\rho_n(T_0)$ and $H_{c2}(T')$ (since $H_{c2}$ does depend on $T'$) into previous equations gives the $j(E)$ response in terms of $T'$:

$$j = v\eta(T')/\Phi_0 = EH_{c2}(T')/\rho_n(T_0)B. \tag{2}$$

[a]An abridged version of this derivation was given elsewhere.[13]

### 3.3. *Critical-parameter field dependencies*

One now has the ingredients for calculating the critical field dependencies in a few steps. The $j(E)$ function of Eq. (2) is non-monotonic since $E$ is multiplied by $H_{c2}(T')$ (or $\eta(T')$) which drops rapidly to zero as $T' \to T_c$ with increasing dissipation. The instability occurs at $dj/dE = 0$, which happens at a certain value $T' = T^*$ where $H_{c2}(T')$ (or $\eta(T')$) drops sufficiently rapidly. $T'$ depends explicitly only on the power density $jE = \eta v^2 B/\Phi_0$ and on quantities that depend on $T'$ itself ($\tau_\epsilon$, specific heat, etc.). Hence at the instability, $j^* E^* = v^{*2}\eta(T^*)B/\Phi_0 = \text{const}$, which gives the critical-parameter field dependencies:

$$v^* \propto 1/\sqrt{B}, \qquad E^* \propto \sqrt{B}, \qquad j^* \propto 1/\sqrt{B}, \qquad \text{and } \rho^* \propto B \tag{3}$$

using $E^* = v^* B$, $j^* = v^* \eta(T^*)/\Phi_0$, and $\rho^* = E^*/j^*$. This gives $v^* \propto 1/\sqrt{B}$ in a natural way, consistent with our measurements in this regime and in contrast to the $B$-independent $v^*$ of the pure LO effect near $T_c$.

### 3.4. *Current-voltage characteristics*

To derive the complete $j(E)$ response and absolute values of critical parameters we calculate $T'$ and insert it into Eq. (2). We take $H_{c2}(0) = 120$ T[17] with the WHH function[18] for interpolation between this $H_{c2}(0) = 120$ and $H_{c2}(T_c) = 0$ (There is some theoretical controversy regarding the exact form of $H_{c2}(T)$; however, empirically, direct measurements[17] of $H_{c2}(T)$, within their uncertainity, seem not to depart drastically from the WHH function, and the exact functional shape does not crucially affect our conclusions.). The dissipation raises the electronic energy by $jE\tau_\epsilon$, which is related to $T'$ by

$$jE\tau_\epsilon \approx \frac{E^2 H_{c2}(T')\tau_\epsilon}{\rho_n(T_0)B} \approx \int_{T_p}^{T'} c(T)dT \approx \int_{T_0}^{T'} c(T)dT \tag{4}$$

where $c(T)$ is the electronic specific heat. Note that $\tau_\epsilon$ can be thought of as being defined by the above equation. It is the ratio of the internal energy (R.H.S. of Eq. (4)) to $jE$, the net energy transfer rate.[b] To calculate $c(T)$, $Y_1Ba_2Cu_3O_{7-\delta}$ is modeled as a layered $d$-wave superconductor: $\Delta_{\vec{k}}(T) = \Delta_0(T)[k_x^2 - k_y^2]/k^2 \approx \Delta_0(T)\cos(2\theta)$, taking the BCS temperature dependence for $\Delta_0(T)$ and $\Delta_0(0) = 19$ meV from tunneling and infrared measurements.[20] Then $c(T) = \partial\{\sum_k E_k f_k\}/\partial T$, where $f_k = [\exp(E_k/k_B T) + 1]^{-1}$ is the Fermi-Dirac distribution, $E_k = \sqrt{\zeta_k^2 + \Delta_k^2}$, $\zeta_k = \epsilon_k - \mu$, and $\mu = 0.2$ eV is the chemical potential.[21] With the replacement

[b]Elsewhere[19] we calculate the net rate of transfer of energy between the quasiparticles and phonons in a superconductor. Near the instability, $T^*$ varies over a small range for different starting $T_0$ values (see Fig. 1) and the derived $\tau_\epsilon$ was found to have an insignificant dependence on this narrow range of final heated electronic temperature, effectively making it a constant in the L.H.S. of Eq. (4). At small values of $T'$ the whole L.H.S. of Eq. (4) is negligible and then the flux flow is in its usual free linear limit, making the (strong) variation of $\tau_\epsilon$ at low temperatures irrelevant.

of $\sum_k$ by $\int d\zeta N(0) \int d\theta/2\pi$ (where $N(0)$ is the normal density of states at $\mu$) this $c(T)$ is now inserted into Eq. (4), which is integrated numerically to obtain $T'$ and thence $j(E)$ from Eq. (2).

The numerical results of the above calculation are shown in Fig. 1. The $j(E)$ curves of panel (a) have an infinite slope at the instability ($j^*$, $E^*$), indicated by arrows, and then exhibit negative slope. This negative sloped portion is experimentally forbidden in a current biased measurement and instead will be manifested as a vertical jump in $E$. The electronic temperature $T'$ rises from the bath value $T_0$ to $T^*$ at the instability. Panel (b) shows the computed $T^*$, which is independent of $B$ as expected but has a slight dependence on the bath temperature $T_0$.

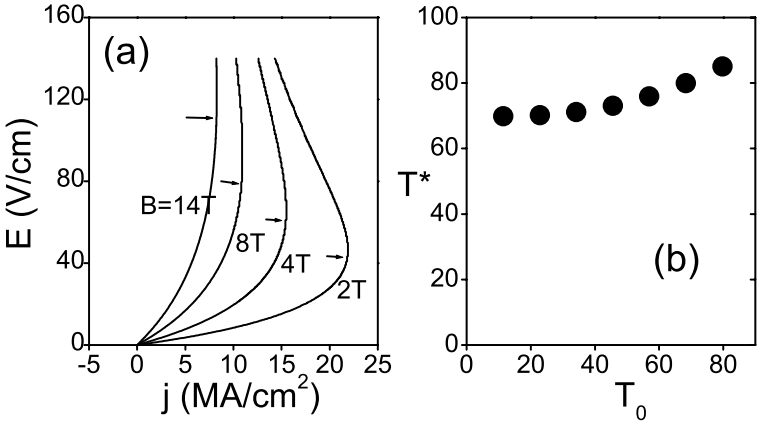


Fig. 1. Numerical results obtained from solving Eq. (4), as described in the text. (a) Theoretical $j(E)$ curves, at $T_0$= 0 K. The onset of negative slope, indicated by arrows, marks the instabilities. (b) The critical temperature $T^*$ for different initial temperatures $T_0$; $T^*$ is independent of $B$ and $\tau_\epsilon$.

In order to conveniently scale the experimental curves, the exact numerical $j(E)$ function derived above — and plotted in Fig. 1 — can be cast into a mathematically more manageable form by noting that the R.H.S. of Eq. (4) can be approximated by $jE\tau_\epsilon \approx \Delta(T')n_q(T') - \Delta(T_p)n_q(T_p) \approx \Delta(T')n_q(T')$. $\Delta$ and $n_q$ are connected through the statistical equations of the previous paragraph. Numerically computing the number of quasiparticles excited above the gap (taking the anisotropic $d$-wave gap together with a BCS temperature dependence as discussed above) we obtain the following $d$-wave generalization of the $\Delta - n_q$ relationship: $(\Delta/\Delta_0)^2 = f(n_q/n)$, where $n = 2.7 \times 10^{21}$ cm$^{-3}$ is the carrier concentration and $f(x) \simeq 1 - 0.4386x - 1539x^2 + 40381x^3 - 345217x^4$ (despite the appearance of successively increasing coefficients in $f(x)$, the terms rapidly converge because $x = n_q/n \sim k_BT/E_F \sim 0.01$). Combining this with the earlier $jE\tau_\epsilon \approx \Delta(T')n_q(T')$, $\eta = j\Phi_0/v = j\Phi_0 B/E$, $\eta \approx H_{c2}\Phi_0/\rho_n$, and $\eta \propto \Delta$, we get a convenient closed form for the non-linear $j(E)$

characteristic:

$$j \approx \left(\frac{H_{c2}(T_0)}{B\rho_n(T_0)}\right) E\sqrt{f(x)} \tag{5}$$

with $x = n_q/n = 0.0245 \times E^2/E^{*2}$, and $E^* = \sqrt{0.0245\rho_n(T_0)Bn\Delta_0/\tau_\epsilon H_{c2}(T_0)}$ is the value of $E$ at the instability peak.

### 3.5. *Critical resistivity*

From the two left components of Eq. (4) one can write down an expression for the critical resistivity $\rho^* = E^*/j^*$ at the instability point:

$$\rho^* = \rho_n B/H_{c2}(T^*) \simeq \gamma\rho_f \tag{6}$$

where $T^*$ was obtained numerically from Eq. (4) and plotted in Fig. 1(b), and $\rho_f$ is the free-flux-flow resistivity in the linear limit (Eq. (1)). This result shows that $\rho^*$ like $\rho_f$ should be proportional to $B$ (as deduced earlier — see Eq. (3)) and that the two are related by a factor $\gamma$, which turns out to be of order unity (since $T^*$ does not depend on $B$, neither does $\gamma$). Figure 2(a) shows the numerically computed $\gamma$ found from Eq. (6) and the computed $T^*$ (Fig. 1(b)). Over the temperature range of interest, $\gamma \sim 2$ so that the critical resistivity is about twice the free-flux-flow value.

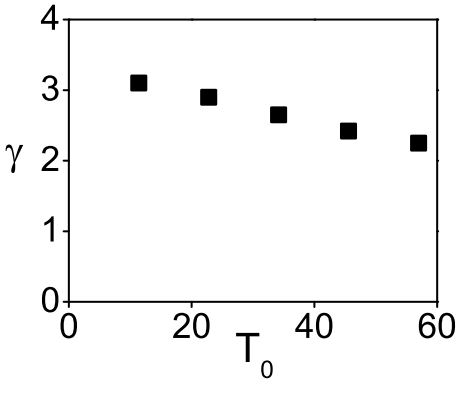


Fig. 2. Numerically computed scale factor $\gamma$ ($= \rho^*/\rho_f$) that relates the critical resistivity (the resistivity at the instability peak) to the free-flux-flow value (see Eq. (6)). $\gamma$ is independent of $B$ but shows a slight variation with the bath (phonon) temperature.

## 4. Experimental Details

All measurements were made on $c$-axis oriented epitaxial films of $Y_1Ba_2Cu_3O_{7-\delta}$ on (100) $LaAlO_3$ substrates with $T_c$'s around 90 K and of thickness $t \approx 90$ nm. Electron-beam lithography was used to pattern bridges of widths $w \approx 2$–$20$ $\mu$m and

lengths $l \approx 30$–$200$ $\mu$m. Altogether ten samples were studied at 12 temperatures (1.6, 2.2, 6, 7, 8, 10, 20, 27, 35, 42, 50, 80 K) and at 13 flux densities (0.1, 0.2, 0.5, 1, 1.5, 2, 10, 11, 13, 13.5, 13.8, 14, 15.8 T). The electrical transport measurements were made with a pulsed constant current source, preamplifier circuitry, and a digital storage oscilloscope. The pulse rise times are about 100 ns with a duty cycle of about 1 ppm, which for the narrowest bridges result in effective thermal resistances of order 1 nK.cm$^3$/W. Note that the $j$ values in the experiment are an order of magnitude lower than the depairing current density[22] and the applied flux densities exceed the self field of the current by at least two orders of magnitude. Further details about the experimental techniques are discussed elsewhere.[23,24]

## 5. Results and Analysis

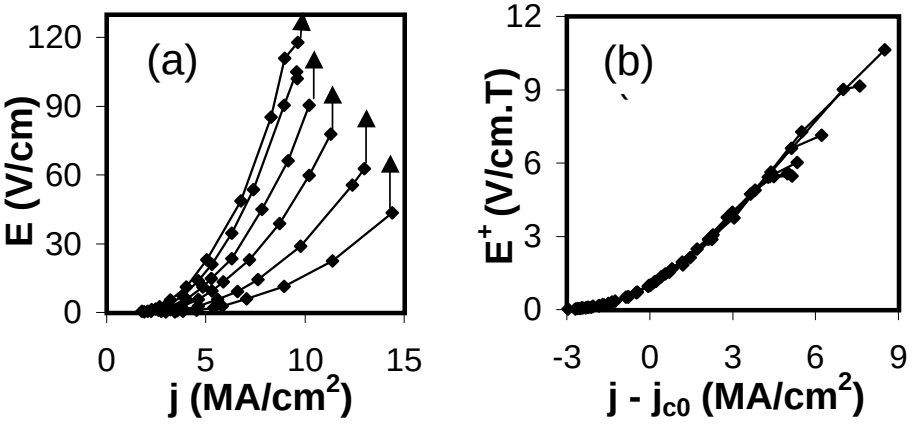


Fig. 3. Experimental current-voltage characteristics. (a) Raw values of $E$ versus $j$ at $T = 20$ K and applied $B$ values of (from lowest to highest curve) 3, 5, 8, 11, 13.8, and 15.8 T. The last symbol on each curve is right at the instability. The slightest further increase of $j$ (entering the forbidden negative-sloped portion of the theoretical curves of Fig. 1) causes $E$ to make discontinous vertical jumps (arrows). (b) The same data plotted as $E^+ = (E/B) \times \sqrt{f(0.0245E^2/E^{*2})}$ (as per Eq. (5)) versus $j - j_{c0}$, where the critical depinning current density $j_{c0}$ is defined at $E^+ = 1$ V/cm.T (the scaling is not affected by the choice of criterion).

Figure 3(a) shows a typical set of experimental $j(E)$ curves. The last stable datapoint ($j^*$, $E^*$) of each curve is at the tail of each arrow. The slightest further increase of $j > j^*$ causes a drastic vertical jump in $E$ as shown by the arrows (the voltage pulse jumps off the scale of the oscilloscope up to the compliance limit of the current source). The jumps show only a small hysteresis $< 3\%$ of $j^*$. (As expected for a current-biased measurement, the break occurs slightly before the slope has become quite vertical.[12]) Figure 3(b) shows the same data plotted as the R.H.S. of Eq. (5) vs $j - j_{c0}$, the excess current density over the depinning value. The data

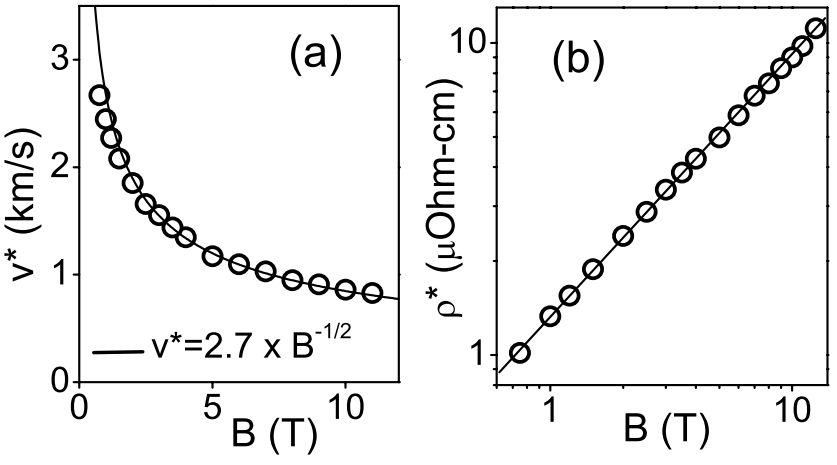


Fig. 4. Variation of critical parameters with flux density. The measurements were made at $T = 1.6$ K. (a) The critical velocity shows a $v^* \propto 1/\sqrt{B}$ trend (solid line is a $1/\sqrt{B}$ fit). (b) The critical resistivity is proportional to the flux density (straight line is a guide to the eye).

scale well and tend toward homogeneous linearity. Note that the collapse implies an excellent proportionality between $\rho$ and $B$ over the entire range.

Figure 4 shows experimentally measured $B$ dependencies of $v^*$ and $\rho^*$ for $T_0 = 1.6$ K, demonstrating excellent agreement with Eq. (3) (the other dependencies $E^* \propto \sqrt{B}$ and $j^* \propto 1/\sqrt{B}$ follow from $\rho^* \propto B$ and $v^* \propto 1/\sqrt{B}$). The $v^* \propto 1/\sqrt{B}$ dependence was found to be ubiquitous for all of our low-$T$ measurements in ten samples (spanning 1.6 K $\leq T \leq$ 50 K and 0.5 T $\leq B \leq$ 15.8 T) and has also been seen by Xiao *et al.*[10] at intermediate temperatures (at the lower end of their $T \sim$ 60–90 K range of study). Note that the excellent linearity between between $\rho^*$ and $B$ demonstrates the independence of $\eta$ on $B$ in this regime; then the resistivity is simply proportional to the number of vortices and hence $B$.

Figure 5(a) shows $\rho_n$ deduced from the measured critical resitivity and $\gamma$ (Fig. 2). Figure 5(b) shows $\rho_n$ found by Nakagawa *et al.*[17] by quenching the superconductivity with high magnetic fields. The latter is subject to errors due to magnetoresistance corrections and the former subject to inaccuracies in our instability model. However both show comparable trends in $\rho_n(T)$ allowing for some magnetoresistance shifts. Together the two results show that the basic nature of flux flow, at least in the YBCO cuprate superconductor, is relatively conventional over the entire temperature range and that the normal-state has metallic residual value in the $T \to 0$ limit, as it is for ordinary low-$T_c$ superconductors.

## 6. Conclusion

In conclusion, we investigated flux flow over the entire temperature range in the YBCO cuprate superconductor and found that the basic nature of flux flow is rela-

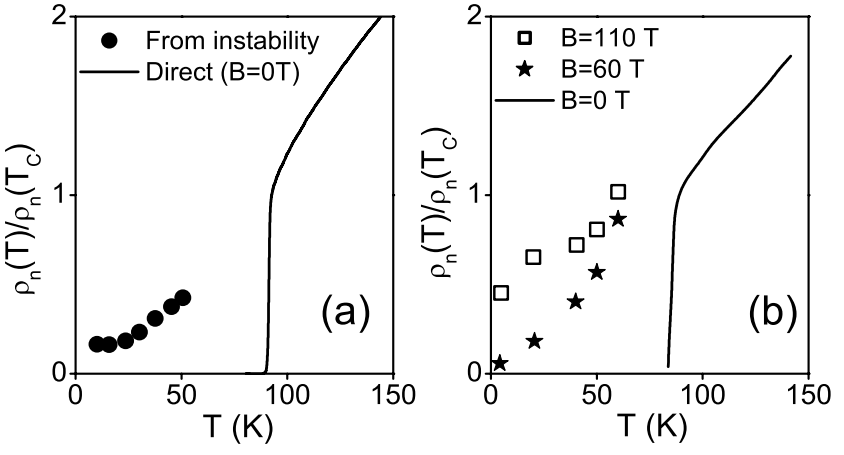


Fig. 5. The normal-state resistivity versus temperature (a) as deduced from the flux-flow instability of the present work and (b) from high-field transport measurements by Nakagawa *et al.* The results are comparable, allowing for some magnetoresistance correction, and togther show that the nature of flux flow is conventional over the entire temperature range and that the normal state has a coventional metallic character.

tively conventional with a magnitude similar to Bardeen-Stephen. The normal-state resistivity deduced from the flux flow is consistent with a direct transport measurement at high fields larger than $H_{c2}$. When the flux motion is driven far beyond free flux flow, we observe an instability under all conditions of fields, and temperatures from $\sim T_c/2$ down to essentially $T \approx 0$. The nature of this low-temperature instability seems to be well described by a model where the electron gas is heated above the phonon temperature leading to the generation of quasiparticles and loss in viscosity as the vortex core expands and $\Delta$ is reduced. This scenario is different from the standard LO picture (dominant mainly near $T_c$) where the vortex shrinks and quasiparticles leave its vicinity. Because the present effect prevails even at temperatures well below $T_c$ (where most superconductive devices operate) it becomes an important consideration in the design of applications where the superconductor operates in the dissipative regime, since the instability triggers an abrupt rise in dissipation at $j$ values much below the depairing current density.

## Acknowledgements

The authors gratefully acknowledge useful discussions and other assistance from B. I. Ivlev, M. Geller, D. K. Christen, J. M. Phillips, R. P. Huebener, N. Schopohl, J. Blatter, and V. Geshkenbein. This work was supported by the U. S. Department of Energy through grant number DE-FG02-99ER45763.

## References


1. A. I. Larkin and Yu. N. Ovchinnikov, in *Nonequilibrium Superconductivity*, eds. D. N. Langenberg and A. I. Larkin (Elsevier, Amsterdam, 1986), Ch. 11.
2. J. Bardeen and M. J. Stephen, *Phys. Rev.* **140**, A1197 (1965); M. Tinkham, *Phys. Rev. Lett.* **13**, 804 (1964); and J. R. Clem, *Phys. Rev. Lett.* **20**, 735 (1968).
3. N. B. Kopnin and G. E. Volovik, *Phys. Rev. Lett.* **79**, 1377 (1997).
4. A physically intuitive discussion can be found in Michael Tinkham, *Introduction to Superconductivity*, 2nd Edition (McGraw Hill, New York, 1996).
5. M. N. Kunchur, D. K. Christen, and J. M. Phillips, *Phys. Rev. Lett.* **70**, 998 (1993).
6. A. I. Larkin and Yu. N. Ovchinnikov, *Zh. Eksp. Teor. Fiz.* **68**, 1915 (1975) [*Sov. Phys. JETP* **41**, 960 (1976)].
7. W. Klein, R. P. Huebener, S. Gauss, and J. Parisi, *J. Low Temp. Phys.* **61**, 413 (1985).
8. L. E. Musienko, I. M. Dmitrenko, and V. G. Volotskaya, *Pis'ma Zh. Eksp. Teor. Fiz.* **31**, 603 (1980) [*JETP Lett.* **31**, 567 (1980)]; and A. V. Samoilov *et al.*, *Phys. Rev. Lett.* **75**, 4118 (1995).
9. S. G. Doettinger *et al.*, *Phys. Rev. Lett.* **73**, 1691 (1994).
10. Z. L. Xiao *et al.*, *Phys. Rev.* **B53**, 15265 (1996).
11. G. M. Eliashberg, *JETP Lett.* **11**, 114 (1970) [*Sov. Phys. JETP* **34**, 668 (1972)]; and B. I. Ivlev, S. G. Lisitsyn, and G. M. Eliashberg, *J. Low Temp. Phys.* **10**, 449 (1973).
12. A. I. Bezuglyj and V. A. Shklovskij, *Physica* **C202**, 234 (1992).
13. M. N. Kunchur, *Phys. Rev. Lett.*, in press (2002).
14. A. I. Bezuglyj, *Physica* **C323**, 122 (1999).
15. V. G. Voltskaya, *et al.*, *Sov. J. Low Temp. Phys.* **18**, 683 (1993).
16. S. G. Doettinger *et al.*, *Physica* **C251**, 285 (1995).
17. H. Nakagawa, N. Miura, and Y. Enomoto, *J. Phys.: Condens. Matter* **10**, 11571 (1998).
18. N. R. Werthamer, E. Helfand, and P. C. Hohenberg, *Phys. Rev.* **147**, 295 (1966).
19. J. M. Knight and M. N. Kunchur, to be published.
    Preprint at http://www.physics.sc.edu/kunchur/papers/taue.pdf
20. W. Lanping *et al.*, *Phys. Rev.* **B40**, 10954 (1989); and R. T. Collins *et al.*, *Phys. Rev. Lett.* **59**, 704 (1987).
21. C. Poole, H. A. Farach, and R. J. Creswick, *Superconductivity* (Academic Press, San Diego, 1995).
22. M. N. Kunchur, D. K. Christen, C. E. Klabunde, and J. M. Phillips, *Phys. Rev. Lett.* **72**, 752 (1994).
23. M. N. Kunchur, *Mod. Phys. Lett.* **B9**, 399 (1995).
24. M. N. Kunchur, B. I. Ivlev, D. K. Christen, C. E. Klabunde, and J. M. Phillips, *Phys. Rev. Lett.* **84**, 5204 (2000).
25. NIST WebHTS Database, http://www.ceramics.nist.gov/srd/hts/htsquery.htm